

# NONLINEAR SPECTROSCOPY OF INFRARED MULTIPHOTON EXCITED MOLECULES

ERIC MAZUR and CHENG-ZAI LÜ  
*Harvard University, Cambridge MA 02138*

## ABSTRACT

This paper presents an overview of recently obtained results on infrared multiphoton excited molecules using coherent anti-Stokes Raman spectroscopy. The data underline the important role of collisions in the excitation process.

It is a great pleasure and honor to contribute to this volume published in honor of Nicolaas Bloembergen's 70th birthday. Both of us have had the privilege of working with Nicolaas Bloembergen (EM from 1982 to 1984, CZL from 1988 to date). This paper is a tribute to his great knowledge and insights in physics, and is related to two areas that he has much contributed to: nonlinear optics and infrared multiphoton excitation. The work described here was largely inspired by him and the scope of this paper is to present new experimental information supporting a model published by Bloembergen and Yablonovitch in 1978.<sup>1</sup>

## 1. Introduction

Soon after it was found that a polyatomic molecule can be highly vibrationally excited with short intense infrared laser pulses<sup>2</sup> Bloembergen and Yablonovitch formulated the *quasicontinuum model*.<sup>1</sup> According to this model the molecule is initially coherently excited through the low-lying vibrational levels. As the energy in the resonant mode increases, the density of states rises rapidly until the rotationally and power broadened states create a wide, quasicontinuous region of states. Transitions in this region obey Fermi's Golden Rule and are described in terms of rate equations.

Most experimental work to date has been focused on dissociation yields, average number of photons absorbed and product energy distributions. Relatively little is known, however, about the discrete vibrational levels below the quasicontinuum, even though these states play a crucial role in the infrared multiphoton excitation process. In general, the vibrational distributions after infrared multiphoton excitation are hard to study experimentally, because of the fast vibrational relaxation, the inhomogeneous broadening resulting from anharmonic couplings, and the small population of the individual levels at high excitation.

The purpose of this paper is to review information obtained on the excitation process through these low-lying states using nonlinear spectroscopy. Two different types of molecular systems are discussed: one is a small triatomic molecule, OCS, with only a

few degrees of freedom, the other a larger polyatomic molecule, SF<sub>6</sub>. In both cases intermolecular transfer of energy via collisions is shown to play a much more important role than hitherto suspected. Part of the results referred to here have been published previously.<sup>3</sup>

## 2. Experimental

A detailed description of the setup can be found in Ref. 3. Briefly, we use 100-ns pulses from a 10-Hz grating-tuned TEA CO<sub>2</sub>-laser focused down to a 100- $\mu$ m spot size by a 0.15-m focal length cylindrical lens to pump the gas molecules. The CO<sub>2</sub>-laser pulses can be truncated to a shorter, 40-ns duration using a self-triggered plasma-shutter.<sup>4</sup> The experiments were carried out in bulk samples and in a pulsed supersonic beam at variable distance  $x$  from a nozzle of diameter  $D = 0.94$  mm. The vibrational population distribution after infrared multiphoton excitation is measured by a multiplex CARS technique.<sup>5</sup> The probe pulse duration is 8 ns. The multiplex signal, which allows one to obtain the entire spectrum in a single laser shot, is analyzed using a 1-m spectrograph and a Hamamatsu streak camera that is triggered by the (truncated) CO<sub>2</sub>-laser pulse. A number of laser shots at varying time-delays is overlapped on a single streak camera image, yielding three-dimensional information of intensity versus wavelength and time-delay.

Collisions enhance the infrared multiphoton excitation because of collisional broadening and rotational hole-filling during the excitation. In the bulk one can study infrared multiphoton excitation under nearly collisionless conditions by reducing the density of the sample and the duration of the laser pulses. A more efficient way to control collisions, however, is to expand the molecules in a supersonic beam. As the distance  $x$  from the nozzle increases, the translational temperature of molecules decreases, and the mean free time between collisions becomes larger. The translational temperature  $T_i$  in the beam in terms of the Mach number  $M$  is given by:<sup>6</sup>

$$T_i = \frac{T_o}{1 + \frac{1}{2}(\gamma-1) M^2}, \quad (1)$$

where  $T_o$  is the reservoir temperature,  $M$  the Mach number and  $\gamma$  the specific heat ratio. The Mach number can be obtained from an empirical relation:<sup>7</sup>

$$M = A \left( \frac{x-x_o}{D} \right)^{\gamma-1} - \frac{1}{2} A^{-1} \frac{\gamma+1}{\gamma-1} \left( \frac{x-x_o}{D} \right)^{1-\gamma}. \quad (2)$$

The constants  $A$  and  $x_o$  depend only on the specific heat ratio  $\gamma$ . Values for these constants can be found in the literature.<sup>8</sup> The collision frequency of the molecules,  $Z_{\text{beam}}$ , is then obtained from<sup>9</sup>

$$Z_{\text{beam}} = \sqrt{2} n_o \sigma \overline{v_o} \left[ 1 + \frac{1}{2}(\gamma-1) M^2 \right]^{-1/2} (\gamma+1)^{1/2} (\gamma-1)^{-1/2}, \quad (3)$$

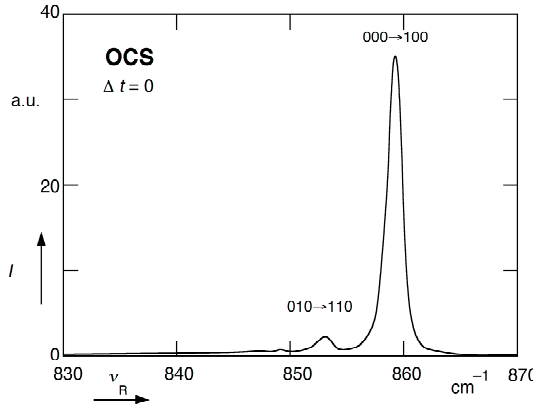


Fig. 1. Coherent anti-Stokes Raman spectrum for OCS at  $T = 300$  K and  $p = 100$  torr.

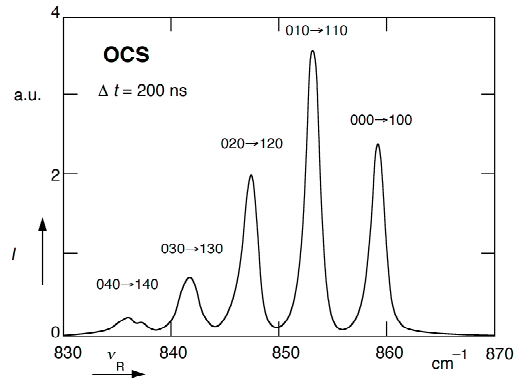


Fig. 2. CARS spectrum for OCS at  $p = 100$  torr, 200 ns after excitation.

where  $n_0$  is the reservoir density,  $\sigma$  the collision cross-section, and  $\overline{v_0}$  the mean velocity of the molecules in the reservoir. As the distance  $x$  is increased, the Mach number increases, and the temperature  $T_i$  and collision frequency  $Z_{\text{beam}}$  decrease.

### 3. OCS

The OCS molecule has three widely separated fundamental modes ( $\nu_1 = 859$   $\text{cm}^{-1}$ ,  $\nu_2 = 527$   $\text{cm}^{-1}$ ,  $\nu_3 = 2079$   $\text{cm}^{-1}$ ). Because of this wide separation, and also because of a low density of states, the intramolecular vibrational energy transfer between modes is very inefficient. In contrast, pumping and population redistribution within the  $\nu_2$  bending mode, excited by the  $\text{CO}_2$ -laser, is very efficient owing to the small anharmonicity,  $x_{22} = 0.35$   $\text{cm}^{-1}$ . The overtone of this mode can be pumped with a  $\text{CO}_2$ -laser with frequencies between the  $P(10)$  and  $P(26)$  lines of the  $9.6$   $\mu\text{m}$  branch. Thus, OCS is an ideal molecule for studying the interaction of a single anharmonic oscillator with an intense infrared laser field.

The experimental results obtained in the bulk<sup>3</sup> are shown in Figs. 1 through 3. The CARS spectrum of the  $\nu_1$  mode of OCS at room temperature is shown in Fig. 1. The peak furthest to the right is the ground state peak, and corresponds to the vibrational transition between the  $(\nu_1, \nu_2, \nu_3) = (0, 0, 0)$  and  $(1, 0, 0)$  states. The second peak from the right reflects the bending hot band  $(0, 1, 0) \leftrightarrow (1, 1, 0)$ , and the barely visible peak furthest to the left is due to the ground state of the  $^{34}\text{S}$  isotope with a 4% natural abundance. The excited state peaks are shifted because of the  $6$   $\text{cm}^{-1}$  cross-anharmonicity between the  $\nu_1$  and  $\nu_2$  modes.

Figure 2 shows the spectrum 200 ns after excitation with a  $9.2\text{-J}/\text{cm}^2$  pulse on the  $9P(24)$   $\text{CO}_2$ -laser line. The ground state peak intensity decreases by more than a factor of 10 (note the difference in scale with Fig. 1), and additional peaks corresponding to excitation in the  $\nu_2$  ladder up to  $\nu_2=4$  appear in the spectrum. The overall time-evolution of the CARS spectrum at 50 torr is shown in Fig. 3. Note the strong ground state signal depletion for times  $t < 1$   $\mu\text{s}$ , and the slow recovery at longer time-delays. In contrast, the other peaks in the  $\nu_2$  hot band grow and then decrease again.

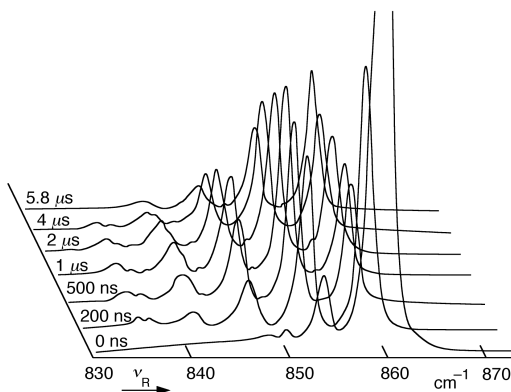


Fig. 3. CARS spectrum for OCS at  $p = 50$  torr, for various delay times after excitation.

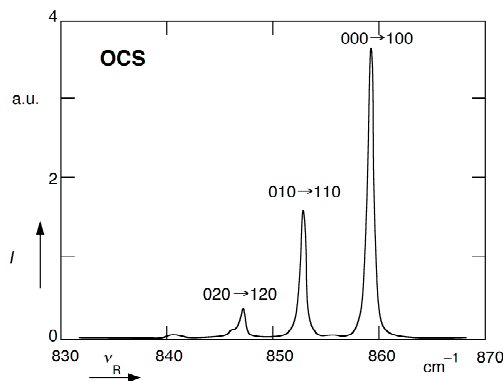


Fig. 4. CARS spectrum for OCS in a molecular beam at  $x/D = 2.6$ , 200 ns after excitation.

From the intensity distribution of the hot band peaks one can obtain the vibrational population distribution in the  $\nu_2$  mode.<sup>3</sup> In the bulk the distribution is always in excellent agreement with a Boltzmann distribution, except at the highest excitation, where small deviations occur. The corresponding temperature of the  $\nu_2$  mode rises for approximately 1  $\mu\text{s}$  before slowly decaying back to its original value. This rise is relatively slow compared to the duration of the  $\text{CO}_2$ -laser pulse and must be attributed to the long 1- $\mu\text{s}$  tail of the laser pulse. In addition, it was found that a higher temperature is obtained at higher sample pressures. For short time-delays the temperature increase is nearly linear with pressure, which implies that the excitation is enhanced by collisional processes. There are two reasons for this collisional enhancement. First, pressure broadening helps compensate for the anharmonicity. Second, because the  $\text{CO}_2$ -laser is resonant with a specific rovibrational transition, the excitation creates a hole in the rotational manifold. Collisions redistribute the population in the rotational manifold, refilling the hole, thereby assisting the excitation and reducing saturation of the pumped transition.

From the time-dependence of the spectra one can obtain information on the vibrational relaxation rates. The fast collisional relaxation of energy within the  $\nu_2$  mode is most clearly reflected by the fact that even though the laser populates the  $\nu_2 = 2$  state, the population of the  $\nu_2 = 1$  state always exceeds the population of the  $\nu_2 = 2$  state. In general, the large population in the odd states implies that the energy transfer rate to those states exceeds the excitation rate. The observed equilibration of energy on a time scale of 100 ns at 10 torr provides a lower limit of  $k_{\nu_2 \nu_2} \geq 1 \mu\text{s}^{-1} \text{ torr}^{-1}$  for the collisional relaxation rate of the  $\nu_2$  mode. As a result of this fast relaxation most spectra reflect a Boltzmann distribution with a well-defined temperature.

As can be seen in Fig. 3, at time-delays longer than 500 ns, extra small peaks appear between the  $\nu_2$  hot band peaks, *e.g.* at 844  $\text{cm}^{-1}$ . These peaks are due to collisional transfer of vibrational energy to the  $\nu_3$  mode and can be assigned to the  $\nu_3$  hot band, *i.e.*  $(0,0,1) \leftrightarrow (1,0,1)$ ,  $(0,1,1) \leftrightarrow (1,1,1)$ , etc. These peaks are displaced from the  $\nu_2$  hot band peaks by the cross-anharmonicity  $x_{13} = -2.7 \text{ cm}^{-1}$ , in good agreement with published values.<sup>10-12</sup> From the appearance of these peaks ( $t \approx 0.5 \mu\text{s}$ ,  $p = 50$  torr), we estimate that

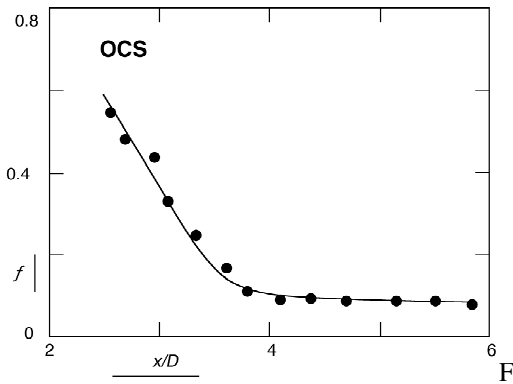


fig. 5. Fraction of excited molecules 200 ns after excitation versus  $x/D$ .

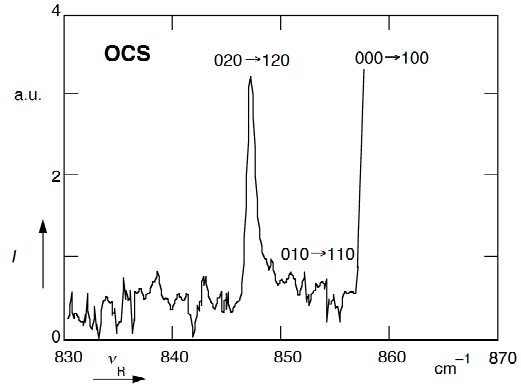


Fig. 6. CARS spectrum for OCS in a molecular beam at  $x/D=3.8$ , 30 ns after excitation.

the energy transfer rate from  $4\nu_2$  to  $\nu_3$  is about  $k_{4\nu_2 \rightarrow \nu_3} \approx 0.04 \mu\text{s}^{-1} \text{ torr}^{-1}$ , a factor of three times faster than reported in the literature.<sup>13</sup>

In the bulk, the dynamics of the vibrational energy distribution is clearly dominated by collisions. Therefore, we also investigated the spectra in a supersonic beam. Close to the nozzle the spectra obtained in the beam resemble the ones obtained in the bulk (see Fig. 4). The peak furthest to the right is again the ground state peak for the  $\nu_2$  mode. As in the bulk, odd-numbered states of the  $\nu_2$  mode are populated because of collisions occurring close to the nozzle in the beam during the laser pulse. Notice that the peaks are narrower because of a dramatic cooling of the rotational distribution.

Farther downstream from the nozzle, the excitation decreases because of the reduced collision rate. This is reflected by a smaller depletion of the ground state for increasing  $x/D$ . The square root of the intensity of this peak is a measure of the number of molecules,  $N_0$ , remaining in the ground state. Figure 5 plots the fraction of excited molecules defined as

$$f = 1 - \frac{N_0}{N}, \quad (4)$$

with  $N$  the total number of molecules, as a function of  $x/D$ . The decrease in excitation clearly shows that, even in a supersonic expansion, collisions contribute to the excitation close to the nozzle. However, if the distance is increased beyond  $x/D > 4$  the excitation no longer decreases. At this distance, where the temperature reaches its lowest point, about 10% of the molecules are still excited under truly collisionless conditions. A spectrum obtained in this regime at a delay of 30 ns is shown in Fig. 6. As expected, the spectrum now only shows a single peak corresponding to the excited overtone level.

For time-delays longer than 60 ns the  $\nu_2=1$  state starts to be populated. This allows us to estimate the energy transfer rate from the pumped overtone state to other levels within the mode. The intensity of the undepleted ground state peak yields a value of  $5 \times 10^{22} \text{ m}^{-3}$  for the density at  $x/D = 3$ . From Eqs. 1 and 2 we obtain a translational temperature of 100

K, yielding a gas-kinetic mean-free-time between collisions of about 120 ns. Therefore, collisional energy transfer occurs within approximately 0.5 gas-kinetic collisions, which corresponds to an energy transfer rate of  $k_{v_2} \varnothing_{v_2} = 15 \mu\text{s}^{-1}\text{torr}^{-1}$  at room temperature.

In the supersonic beam the OCS could only be vibrationally excited by the  $P(22)$  and  $P(18)$  lines of the  $9.6 \mu\text{m}$   $\text{CO}_2$ -laser. This is because in the beam fewer rotational states are populated and there is virtually no collisional broadening. The Rabi frequency for OCS is given by  $\omega_R = 1.3 \times 10^{-5} \sqrt{I}$ , with  $\omega_R$  in  $\text{cm}^{-1}$  and the peak  $\text{CO}_2$ -laser intensity,  $I$ , in  $\text{W}/\text{cm}^2$ .<sup>14</sup> In this experiment one has  $\omega_R = 0.08 \text{ cm}^{-1}$ , and only the  $P(22)$  and  $P(18)$   $\text{CO}_2$ -laser lines have a frequency mismatch below the Rabi frequency. These lines pump the  $P(5)$  and  $R(3)$  transitions of OCS, respectively. This is quite different from the situation in the bulk, where excitation was observed for all  $\text{CO}_2$  lines between the  $P(10)$  to  $P(26)$  lines of the  $9.6 \mu\text{m}$   $\text{CO}_2$ -laser branch. In the bulk, the excitation is enhanced by the broader rotational distribution and rotational hole filling by collisions.

#### 4. $\text{SF}_6$

Despite the fact that overtone pumping is generally weak, the low-lying vibrational levels of OCS are significantly populated by excitation with a short infrared laser pulse. No quasicontinuum states are observed in the spectrum, most likely because of the low density of states of this small molecule. In larger molecules ( $\text{SF}_6$  in particular) extensive efforts have been undertaken to study the spectroscopy and the dynamics of highly vibrationally excited states.<sup>15</sup>

Double infrared resonance was used to study the spectroscopy of  $\text{SF}_6$  under infrared excitation.<sup>16</sup> It was found that two molecular ensembles (one ‘hot’, highly vibrationally excited, one ‘cold’, bottlenecked in the ground state) are formed by infrared multiphoton excitation. Similar results were obtained using spontaneous<sup>17–22</sup> and coherent anti-Stokes Raman scattering.<sup>23</sup> The ‘hot’ ensemble was attributed to a direct observation of the quasicontinuum states, and a number of conclusions regarding the quasicontinuum were drawn based on this assumption. Some of the results for  $\text{SF}_6$ , however, could not be reproduced,<sup>24</sup> and as we will show, a number of the results must be attributed to collisional rather than intramolecular effects.

Here, we study the evolution of the vibrational distribution of  $\text{SF}_6$  in a molecular beam after excitation of the infrared  $\nu_3$ -mode with the  $10P(16)$   $\text{CO}_2$ -laser line. This is done by measuring the coherent anti-Stokes Raman spectrum from the  $\nu_1$ -mode. Again the distance  $x/D$  is varied to allow fine control of the contribution of collisional effects. The collision frequency for different  $x/D$  can be obtained from Eqs. 2 and 3.

Figure 7 shows spectra obtained near the nozzle at  $x/D = 2$  for various pump-probe delays. At this distance the collision frequency is about 10 collisions per 100 ns (the time scale of the excitation). At zero delay the spectrum shows only a single peak corresponding to the ground vibrational state. As can be seen, the excitation rapidly depletes the population in this state. At the same time a broad feature in the shape of a

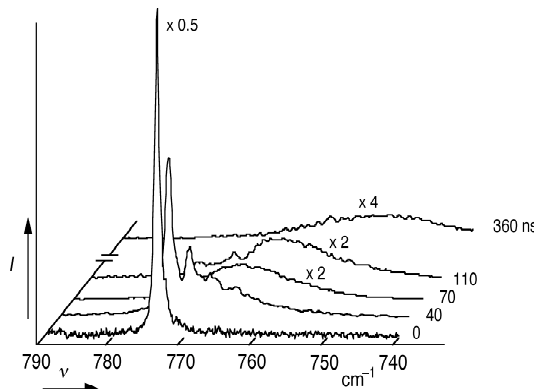


Fig. 7. CARS spectrum for SF<sub>6</sub> in a molecular beam at  $x/D = 2$ , for various time-delays after excitation.

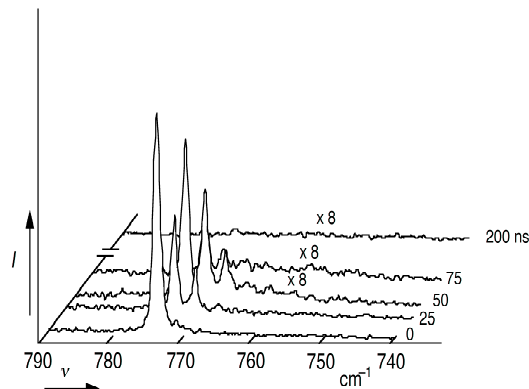


Fig. 8. CARS spectrum for SF<sub>6</sub> in a molecular beam at  $x/D = 10$ , for various time-delays after excitation.

bump appears in the spectrum. Because the CARS signal intensity is proportional to the square of the difference in population between the probed levels, the signal rapidly falls off as this feature and the corresponding distribution of states broaden. A similar feature was observed earlier,<sup>23</sup> and attributed to a high-lying vibrational quasicontinuum of vibrational states at high excitation. One immediately notes, however, that the present measurements show this bump moving towards the right (*i.e.* higher excitation) as time proceeds.

Spectra taken farther downstream, at  $x/D = 10$ , show no such bump at all (see Fig. 8). At this distance we estimate the collision frequency to be about  $10^{-2}$  collisions per 100 ns. Clearly the broad feature observed near the nozzle and in the bulk is not a direct result of infrared multiphoton excitation. Since it only appears when the collision rate is sufficiently high, and since it shifts towards higher excitation as time proceeds, the bump must be attributed to population in intermediate states that results from collisions of ‘cold’ molecules with highly excited ones that are not directly visible in the spectra. These highly-excited states are linear combinations of many normal modes resulting in a very broad, quasicontinuous distribution. Since the CARS signal is proportional to  $\Delta N^2/\Gamma^2$ , with  $\Gamma$  the Raman line width,<sup>25</sup> the signal from these states will become undetectable as the population spreads out.

The existence of these undetected highly-excited molecules is further confirmed by the rapid decrease of the integrated CARS signal. Figure 9 shows the integrated area under the square root of the spectrum as a function of time for the two series of measurements shown in Figs. 7 and 8. This area is a measure for the total number of molecules observed. The area has been normalized to one at zero time-delay and decreases rapidly down to nearly zero for  $x/D = 10$  and to 0.3 for  $x/D = 2$ . This decrease cannot be attributed to dissociation, since the fraction of dissociated molecules at the employed fluence of 0.4 J/cm<sup>2</sup> is less than 0.001<sup>26</sup> (the average number of infrared photons absorbed is only 5).<sup>14</sup>

The excitation thus creates two ensembles: one ‘cold’ near the ground state, visible in the spectrum at large  $x/D$ , and just after excitation for small  $x/D$ , and one broad ‘hot’ ensemble which is *not* directly visible in the CARS spectra. Once the molecules are driven up to these states relaxation is slow, since optical transitions between mixed states are very

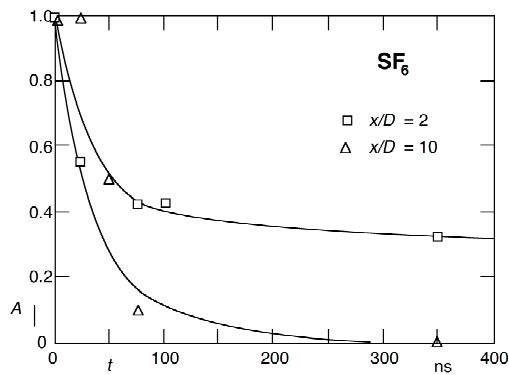


Fig. 9. Integrated area under the square root of the spectra in Figs. 7 and 8 versus time-delay.

weak. Collisions, on the other hand, can efficiently redistribute the energy; at  $x/D = 2$  collisions between the two ensembles created by the excitation result in population of intermediate states ( $5000\text{--}8000\text{ cm}^{-1}$ ). It is these intermediate states that show up in the spectrum as a bump which shifts towards higher excitation as energy relaxes from the highly excited ensemble to lower vibrational levels. It should be emphasized, however, that under collisionless conditions these intermediate states are not observed (Fig. 8), indicating that the population of these intermediate levels directly after excitation is very low.

## 5. Conclusions

The measurements reviewed here show that during the infrared multiphoton excitation of OCS and SF<sub>6</sub>, the low-lying vibrational levels of the pumped mode are significantly populated, contrary to previous observations.<sup>24</sup> The absorbed energy is predominantly confined within the pumped mode, and the population distribution of the low-lying levels can be described by a thermal distribution.

Because of collisions and intermolecular relaxation the spectra of infrared multiphoton excited molecules exhibit complex features. For SF<sub>6</sub>, the bump-like feature observed in spontaneous and coherent Raman spectra<sup>19–23</sup> is not a direct result of the CO<sub>2</sub>-laser excitation, but of a combination of inter- and intramolecular vibrational relaxation. Even in a small molecule like OCS, collisions can cause a rapid energy transfer with the pumped mode.

Finally, these results clearly demonstrate the usefulness of coherent anti-Stokes Raman spectroscopy and molecular beam techniques for time-resolved studies of the vibrational distributions in infrared multiphoton excitation and the dynamics of vibrational energy transfer between highly excited states.

## Acknowledgments

We would like to acknowledge the contributions of Dr. Kuei-Hsien Chen, Mr. Shrenik Deliwala and Mr. Jay Goldman, and the many useful discussions with Profs. N. Bloembergen and M.J. Shultz. This work was funded by the Army Research Office

contracts DAAL03-88-K-0114 and DAAL03-88-G-0078, by the Joint Services Electronics Program contract N00014-89-J-1023, and by Hamamatsu Photonics K.K.

## References

1. N. Bloembergen and E. Yablonovitz, *Physics Today* **5** (1978) 23.
2. N.R. Isenor and M.C. Richardson, *Appl. Phys. Lett.* **18** (1971) 224.
3. K.H. Chen, C.Z. Lü, L.A. Avilés, E. Mazur, N. Bloembergen and M.J. Shultz, *J. Chem. Phys.* **91** (1989) 1462.
4. H.S. Kwok and E. Yablonovitch, *Opt. Commun.* **21** (1977) 252.
5. W.B. Roh, P.W. Schreiber and J.P.E. Taran, *Appl. Phys. Lett.* **29** (1976) 174.
6. P.N. Bajaj and P.K. Chakraborti, *Chem. Phys.* **104** (1986) 41.
7. H. Ashkenas and F.S. Sherman, in *Rarefied Gas Dynamics*, ed. J. H. de Leeuw, (Academic Press, New York, 1966), p. 106.
8. J.B. Anderson, *AIAA Journal* **10** (1972) 112.
9. D.M. Lubman, C.T. Rettner and R.N. Zare, *J. Phys. Chem.* **86** (1982) 1129.
10. Y. Morino and T. Nakagawa, *J. Mol. Spectrosc.* **26** (1968) 496.
11. A. Foord, J.G. Smith and D.H. Whiffen, *Mol. Phys.* **29** (1975) 1685.
12. B. Hegemann and J. Jonas, *J. Chem. Phys.* **79** (1983) 4683.
13. M.L. Mandich and G.W. Flynn, *J. Chem. Phys.* **73** (1980) 1265.
14. T.B. Simpson and N. Bloembergen, *Chem. Phys. Lett.* **100** (1983) 325.
15. V.N. Bagratashvili, V.S. Lethokov, A.A. Makarov and E.A. Ryabov, *Multiple Photon Infrared Laser Photophysics and Photochemistry*, (Harwood Acad. Publ., Chur, 1985).
16. R.V. Ambartzumian, N.P. Furzikov, Y.A. Gorokov, V.S. Letokhov, G.N. Makarov and A.A. Puretzky, *Optics Comm.* **18** (1976) 517.
17. E. Mazur, I. Burak and N. Bloembergen, *Chem. Phys. Lett.* **105** (1984) 258.
18. J. Wang, K.H. Chen and E. Mazur, *Phys. Rev. A* **34** (1986) 3892.
19. V.N. Bagratashvili, Y.G. Vainer, V.S. Doljnikov, S.F. Koliakov, A.A. Makarov, L.P. Malyavkin, E.A. Ryabov, E.G. Silkis and V.D. Titov, *Appl. Phys.* **22** (1980) 101.
20. V.N. Bagratashvili, V.S. Doljnikov, V.S. Lethokov, A.A. Makarov, L.P. Maljavkin, E.A. Ryabov, E.G. Silkis and Y.G. Vainer, *Opt. Comm.* **38** (1981) 31.
21. V.N. Bagratashvili, Y.G. Vainer, V.S. Doljnikov, V.S. Lethokov, A.A. Makarov, L.P. Malyavkin, E.A. Ryabov and E.G. Silkis, *Opt. Lett.* **6** (1981) 148.
22. V.N. Bagratashvili, Y.G. Vainer, V.S. Dolzhikov, S.F. Kol'yakov, V.S. Letokhov, A.A. Makarov, E.A. Ryabov, E.G. Sil'kis and V.D. Titov, *Sov. Phys. JETP* **53** (1981) 512.
23. S.S. Alimpiev, S.I. Valyanskii, S.M. Nikiforov, V.V. Smirnov, B.G. Sartakov, V.I. Fabelinskii and A.L. Shtarkov, *JETP Lett.* **35** (1982) 361.
24. J.I. Steinfeld, *Spectrochimica Acta* **43A** (1987) 129.
25. Y.R. Shen, *The principles of nonlinear optics*, (Wiley & sons, New York, 1984).
26. T.B. Simpson, J.G. Black, I. Burak, E. Yablonovitch and N. Bloembergen, *J. Chem. Phys.* **83** (1985) 628.